12-15-1997

Electro-Deposition of Polymer Chains on an Adsorbing Wall: Density Profiles and Wall Coverage

Grace M. Foo
National University of Singapore

Ras B. Pandey
University of Southern Mississippi

Electro-deposition of polymer chains on an adsorbing wall: Density profiles and wall coverage

Grace M. Foo
Supercomputing and Visualization Unit, National University of Singapore, Singapore 119260

R. B. Pandey
Program in Scientific Computing and Department of Physics and Astronomy, University of Southern Mississippi, Hattiesburg, Mississippi 39406-5046

(Received 30 May 1997; accepted 11 September 1997)

Growth of polymer density in an electro-deposition model of polymer chains on an impenetrable wall is studied on a two dimensional discrete lattice using a Monte Carlo simulation. Polymer-polymer repulsion and polymer-wall attraction for the adsorbing wall (along with the neutral and repulsive interactions) are considered in an external field. Effects of the field strength (B), temperature (T), and chain length (L_c) on the density profile of the polymer chains and wall coverage are investigated. The spatial density profile shows onset of oscillation near the wall at a characteristic field (B_c) which depends on chain length and temperature. In low field, adsorption-to-desorption transition at the wall appear on increasing the temperature (unlike neutral and repulsive walls). In high field regime, on the other hand, a non-monotonic dependence of coverage on temperature is observed with a maximum at a temperature (T_m) which increases on increasing B. The equilibrium value of the polymer density (p_d) shows a power-law decay with the chain length, $p_d \sim L_c^{-\alpha}$, at the wall and in the bulk with corresponding values of the exponent α_W and α_B; these exponents differ substantially and depend on B, T, and L_c. The coverage decays monotonically with the chain length at a constant temperature and field. © *1997 American Institute of Physics.* [S0021-9606(97)51347-X]

I. INTRODUCTION

Fundamental understanding of deposition and surface growth processes has enormous applications in a variety of industries such as manufacturing of semi-conductor devices, coatings, paints, composites, and other materials.[1–7] For example, paint-particulates (aggregates or polymer chains) are driven by pressure gradient toward a surface in a spray painting process, while the biopolymers (DNA, RNA, or protein) are driven by electric field in an electrophoretic process leading to DNA finger printing. When the polymer chains are driven by a field, their motion tends to cease or slow down as they encounter barriers (i.e. the surface as an idealized case). In fabricating a thin film, layered material, or in electroplating processes, constituent molecular species are driven by a field toward a target. Deposition of such molecular species tend to alter the original morphology of the target (surface/line) area. Consequently the density of the growing surface layers depends on the details of the process and parameters such as the magnitude of the field, shape and size of the molecular species, temperature, etc. Since analytical treatment is difficult and limited, particularly in the case of extensible structures such as polymer chains, computer simulations provide a useful tool to study such processes.[8–11]

Several attempts have been made in recent years to understand the conformation of polymer chains and their density profile at the surface.[12–18] However none of these studies deal with the growth of the density profiles driven by a field. We use a Monte Carlo simulation method to study the growth of the monomer density along the field (x-)direction and coverage of chains on the wall as the polymer chains are deposited on an impenetrable wall. We investigate the effects of temperature (T), field strength (B) and chain length (L_c) on the density profile of depositing chains. Attempts are made to identify the ranges of B and T which are effective in driving the chains toward the wall that lead to appreciable changes in adsorption and desorption of the chains at the wall.

Over this range of parameters (T, B, and L_c), the problem reduces to a study of polymer chains near an attractive wall, complementing earlier studies of free or attached chains near surfaces or between walls.[12–25] We recover qualitative results similar to some of the earlier simulations while using a simpler model. For example, in low field, we see adsorption transition at low temperatures[19–21] and desorption at high temperature with an adsorption-desorption phase transition at a critical temperature. The adsorption depends on the strength of wall potential (interaction), temperature, and field. In high field, on the other hand, we observe, a non-monotonic dependence of adsorption on temperature with a maximum at a characteristic temperature. For comparison, we also look at the effects of neutral and repulsive walls on the chain behavior. We observe oscillatory behavior of the monomer density profiles near the wall in certain regimes of B and T consistent with previous simulations[21,25] in different contexts. We have also analyzed the conformation of chains in detail and observed interesting crossover in the power-law dependence of the x and y components of the radius of gyration with the chain length from bulk to wall; we offer this report in a separate communication.[26] In the following Sec. II, our chain model is described. The simula-

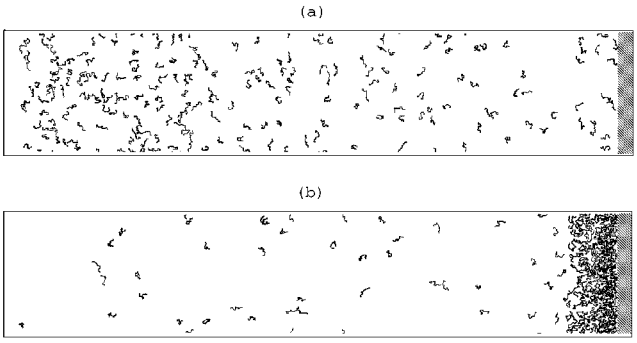

FIG. 1. Snapshot of lattice at 1000 MCS showing configurations of $L_c=40$ chains at (a) $T=100.0$, (b) $T=10.0$, under field of strength $B=2.0$.

tion results are discussed in Secs. III and IV, with a summary in Sec. V.

II. MODEL

We consider self-avoiding walk (SAW) chains on a two-dimensional lattice of size $L_x\times L_y$. We use $L_x=1000$, $L_y=200$ for all the data reported here although we have used various sizes with different aspect ratios (L_x/L_y) to check for the severe finite size effects. At equal time intervals, up to $p\times L_y$ (with $p=0.05$) chains of length L_c are generated at the left end of the lattice ($x=1$ to $x=p\times L_x$), i.e., attempts are made to release chains at a constant rate from the source end. In order to use a nearest neighbor interaction in addition to excluded volume, a positive charge or interaction density ($\rho=1$) is assigned to each polymer node/bead, while the attractive wall (located at $x=L_x$) is made up of a line (length L_y) of negative charges ($\rho=-1$). Neutral ($\rho=0$) and repulsive ($\rho=1$) walls are also considered. Further, we consider an external field of strength B along the positive x-direction. Thus, the interaction energy is described by,

$$E=\sum_{ij}\rho_i\rho_j+B\sum_i\rho_i dx_i, \tag{1}$$

where the first summation is restricted to nearest neighbor sites and $dx_i=0,\pm1$ is the displacement of the ith chain node along the x-direction. Metropolis algorithm is used to reptate the chains with a periodic boundary condition to move chains across the y boundary. It is worth pointing out that the reptation dynamics (as with many others such as kink-jump, crank-shaft, etc.) is unphysical and is used here primarily to speed up the program to study the profiles of the distribution of the chains. We define one Monte Carlo step (MCS) as $L_x\times L_y$ attempts to reptate randomly selected chains.

The parameters we consider are the chain length L_c, temperature T, and field strength B. Four chain sizes are used in this study, $L_c=40$, 80, 120 and 160. At intervals of 50 MCS for a total of 1000 MCS, up to $0.05\times200=10$ chains are generated at the left end of the lattice. While it is easy to maintain a constant generation (supply/release) rate for shorter chains, it is not possible for the longer ones. The final concentration of the chains in the lattice after a sufficiently long deposition time, therefore, depends on the number of chains generated (with a maximum of 200 here) as well as their length. For $L_c=40$ and $L_c=80$ chains, the final concentration is steady at about 4% and 8% respectively, while for $L_c=120$ chains it ranges from 8% to 12% and for $L_c=160$, 6% to 16%. A range of field strengths ($B=0.1,0.5,1,2,5,10$) and temperatures ($T=0.1,0.5,1,5,10,100$) were explored. As in most MC simulations, units for the interaction energy (Eq. (1)), field strength (B), and temperature (T) are arbitrary with field normalized by k_BT and temperature by k_B, the Boltzmann constant. Note that the order of magnitude in the variation of these parameters is relatively large, but it is necessary some times in such model systems. For each set of parameters, $n_s\sim20$ simulations were performed to obtain reliable esti-

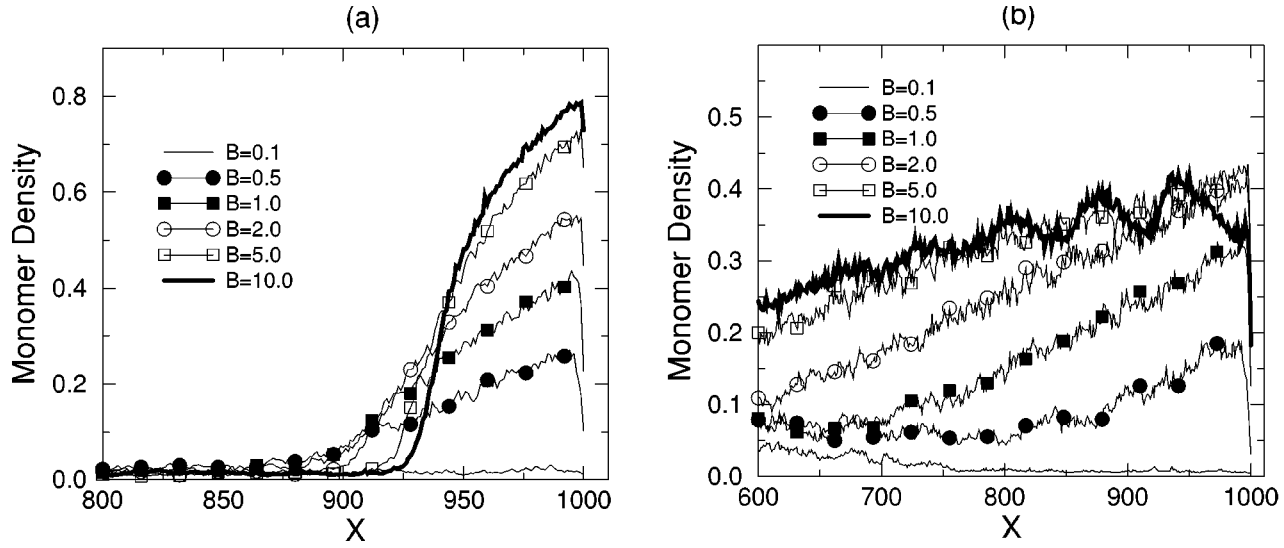

FIG. 2. Monomer density vs X of (a) $L_c=40$, (b) $L_c=160$ chains at $T=10.0$ near the wall.

mates of the physical quantities, i.e., the monomer density along the field (x-)direction and the coverage of chains at the wall.

III. MONOMER DENSITY PROFILES

As described above all the chains are released from the source end of the sample (toward $x=1$) where they are located initially. These chains reptate into the lattice and many of them arrive at the wall in appropriate time which depends on the temperature and field. Interaction between the polymer chains and the wall, along with the magnitude of field and temperature affect the adsorption and desorption during such deposition process. Polymer density evolves in the lattice and after a sufficiently long time the polymer density at the wall approaches a steady (equilibrium) value. Thus the monomer density profiles along the field (x-)direction give an indication of the bulk movement of the polymer chains. These profiles depend strongly on T and B. Snapshots of the chain configurations are useful aids to interpreting our data and we will present a few at the final time step (1000 MCS). We note that at high temperatures ($T=100$), the movements of chains along the x-direction are relatively unaffected by the field (see Fig. 1(a)) in our observation time. Since the energy of the chains (at high T) negates the influence of low fields, i.e., the electrostatic energy due to field, a high field ($B\geqslant 5.0$) is required to drive them toward the wall faster. At lower temperature ($T=10$), the field is more effective in driving the chains and they begin depositing on the wall faster (Fig. 1(b)).

The density profile for chains of length $L_c=40$ is presented in Fig. 2(a) at $T=10$. From Fig. 2(a) we note that the density profiles of $L_c=40$ chains near the wall become increasingly sharp as B increases, i.e., as the field increases more chains are driven toward the wall and they pack more closely together. However at the wall the monomer density decreases. Since the conformations of the chains are restricted at the wall, the chains prefer to avoid it.[21] The density profiles for the long $L_c=160$ chains (Fig. 2(b)) are not only flatter/broader than the corresponding profiles for $L_c=40$ chains but also significantly different in other aspects. For example, the longer chains are not able to pack as close together as the shorter ones near the wall (see Fig. 3(a) and compare with Fig. 1(b)). Note that the steric hindrance leads to some screening, i.e., the entropic constraints become more effective for the long chains. Secondly, at high field $B=10$, we observe oscillations in the density near the wall for these chains unlike for shorter ones. We would like to point out that the oscillatory behavior in the density profiles are also observed in different contexts. For example, the pressure from chains in the bulk and wall constraints induces a layering effect on the monomers.[21] In our study here, the field aligns the chains along x-direction (Fig. 3(b)). The elongated chains see the wall mainly through the end nodes. Chains attached to the wall via their end nodes form polymer brushes in their low entropic energy conformations (due to polymer-polymer repulsion). This induces perturbation on the distribution of adjacent chains leading to oscillations in the density profile (Fig. 2(b)). Further, we see a sharp increase in density both near the source end where the chains are released and near the wall into the bulk, i.e., the dispersion in the polymer density increases on increasing the chain length.

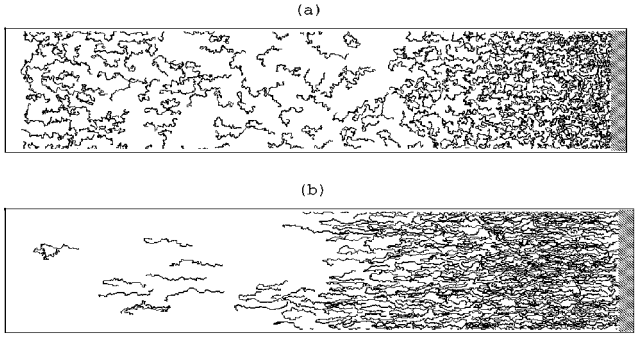

FIG. 3. Snapshot of lattice at 1000 MCS showing configurations of $L_c=160$ chains at $T=10.0$, under field of strength (a) $B=2.0$, (b) $B=10.0$.

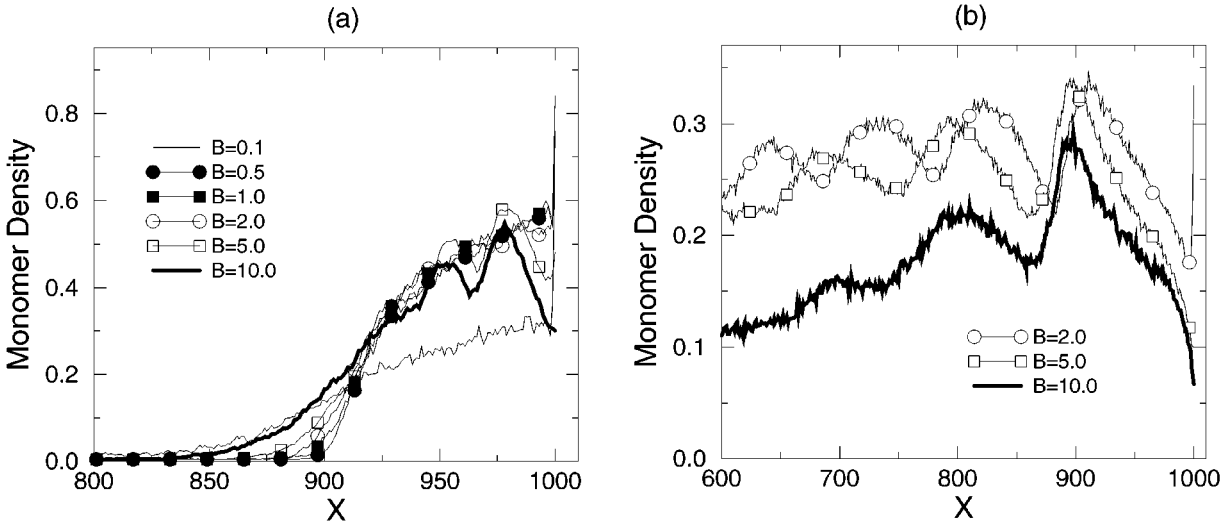

FIG. 4. Monomer density vs X of (a) $L_c=40$, (b) $L_c=160$ chains at $T=1.0$ near the wall.

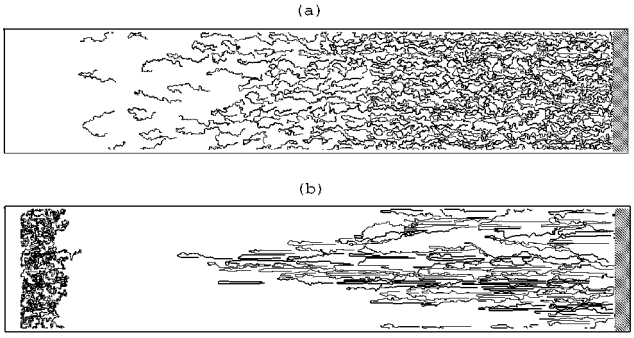

FIG. 5. Snapshot of lattice at 1000 MCS showing configurations of $L_c=160$ chains at (a) $T=1.0$, (b) $T=0.1$, under field of strength $B=0.5$.

At low temperatures ($T=1,2$), the chains reach the wall even at fairly low B in our observation time (Fig. 4). Within a range of low field values, i.e., $B=0.1$ to $B=2.0$ for $L_c=40$, and $B=0.5,1.0$ for $L_c=160$ chains, the monomer density increases very rapidly at the wall. The snapshot of these chains (Fig. 5(a)) reveals that the chains are adsorbed along the wall (along y-direction) in contrast to their conformations near the wall. More segments of the approaching chains feel the wall since the field is too weak to align the chains. For an attractive wall, the chains subsequently adsorb on the wall since it is energetically favourable. At sufficiently high values of B, we observe oscillations in the density profiles similar to those mentioned above for $L_c=160$ chains. Note that we also observe such oscillations at low T for the shorter chains (Fig. 4(a)) unlike their density profile at $T=10$ (Fig. 2(a)). Thus, the characteristic value B_c of the field for the onset of oscillations varies with chain length and temperature; it tends toward larger values as the chain length decreases (at the same T). For example, for $L_c=40$ chains, oscillations are observed for $B=5$ at $T=2$, and for $B=2$ at $T=1$. But for the longer $L_c=120,160$ chains, oscillations occur for $B=2$ and $B=1$ at the corresponding temperatures. The oscillations for the longer chains weaken at very high field ($B=10$) since fewer of them are able to reach the walls at low T (see Fig. 4).

The trend of increasing density on the wall at low field persists at lower temperatures. For example, at very low temperatures ($T=0.1$), high values of the monomer density at the wall are observed at low B (Fig. 6). However, unlike at $T=1$ above, there are oscillations in the monomer densities at these B, i.e., $B=0.5$ to $B=2$ for $L_c=40$ chains and $B=0.5,1$ for $L_c=160$ chains. Away from the wall, the chains at these temperatures are strongly aligned along the x-direction even at low fields (Fig. 5(b)), thus contributing to a layering effect discussed above. Adjacent to wall (at $X=999$) the monomer density drops sharply. But at the wall the energy function becomes important at these temperatures, and we see that the chains are strongly absorbed on it (Table I). They are almost completely aligned with the wall becoming one dimensional chains in the transverse (y-)direction. This is consistent with earlier simulation studies.[19–21] A detailed analysis of the conformational behavior near the wall will be published else where.[26] However, the field is less effective in driving the chains toward the wall and fewer chains (particularly the longer ones) are able to reach it. The oscillations are therefore weaker here than at $T=1$. At very high B the effect is severe, many chains are locked in near the point of generation before reaching the wall. Thus, we see that oscillations in density profile (i.e., layering in monomer distribution) near the wall occur due to rate of growth in polymer density caused by the interplay between the field and temperature along with the chain length.

A. Comparison with neutral and repulsive walls

We perform simulations using neutral ($\rho=0$) and repulsive ($\rho=1$) walls mainly in two parameter spaces: high

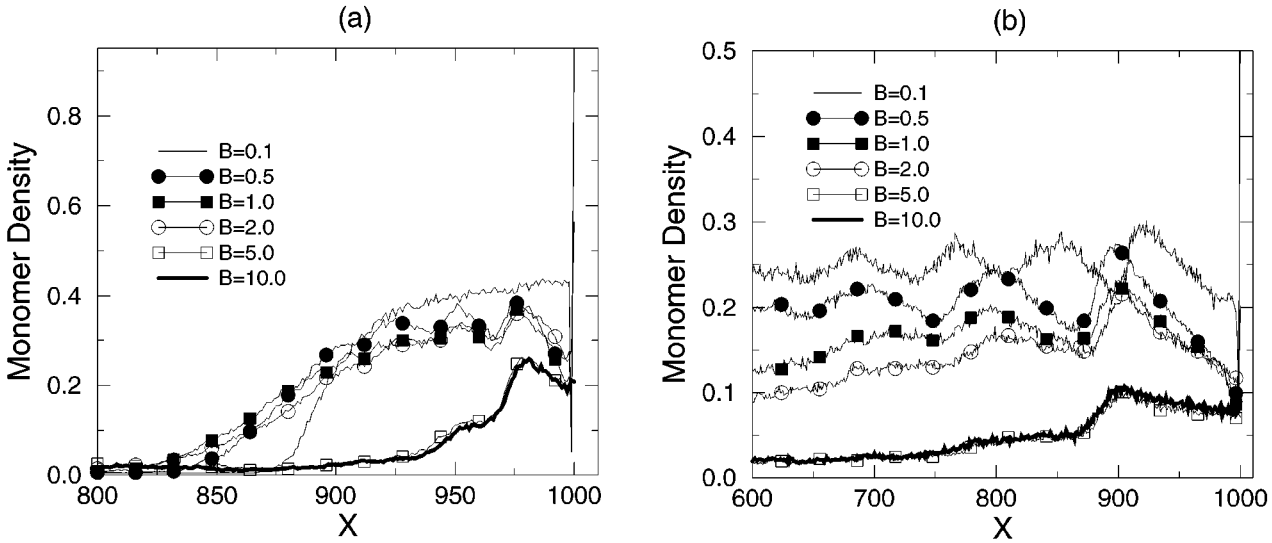

FIG. 6. Monomer density vs X of (a) $L_c=40$, (b) $L_c=160$ chains at $T=0.1$ near the wall.

TABLE I. Monomer density near attractive, neutral and repulsive walls. Error bar on the order of ± 0.03.

X	T	B	L_c	Attractive	Neutral	Repulsive
998	10.0	5.0	40	0.704	0.729	0.712
999	10.0	5.0	40	0.735	0.716	0.71
1000	10.0	5.0	40	0.652	0.612	0.586
998	10.0	5.0	80	0.623	0.615	0.62
999	10.0	5.0	80	0.632	0.613	0.59
1000	10.0	5.0	80	0.509	0.477	0.407
998	10.0	5.0	120	0.517	0.521	0.523
999	10.0	5.0	120	0.493	0.461	0.457
1000	10.0	5.0	120	0.365	0.283	0.263
998	10.0	5.0	160	0.415	0.399	0.383
999	10.0	5.0	160	0.37	0.345	0.323
1000	10.0	5.0	160	0.252	0.207	0.168
998	1.0	0.5	40	0.564	0.566	0.599
999	1.0	0.5	40	0.541	0.607	0.638
1000	1.0	0.5	40	0.84	0.613	0.25
998	1.0	0.5	80	0.42	0.448	0.475
999	1.0	0.5	80	0.448	0.474	0.438
1000	1.0	0.5	80	0.783	0.384	0.089
998	1.0	0.5	120	0.333	0.374	0.346
999	1.0	0.5	120	0.393	0.358	0.29
1000	1.0	0.5	120	0.77	0.243	0.042
998	1.0	0.5	160	0.274	0.3	0.279
999	1.0	0.5	160	0.36	0.272	0.187
1000	1.0	0.5	160	0.747	0.179	0.027
998	0.1	0.5	40	0.276	0.245	0.245
999	0.1	0.5	40	0.111	0.236	0.265
1000	0.1	0.5	40	0.949	0.235	0.007
998	0.1	0.5	80	0.149	0.11	0.119
999	0.1	0.5	80	0.102	0.1	0.119
1000	0.1	0.5	80	0.958	0.097	0.0
998	0.1	0.5	120	0.129	0.079	0.067
999	0.1	0.5	120	0.139	0.073	0.061
1000	0.1	0.5	120	0.954	0.069	0.0
998	0.1	0.5	160	0.102	0.073	0.058
999	0.1	0.5	160	0.126	0.067	0.053
1000	0.1	0.5	160	0.946	0.07	0.0

$T(\geqslant 5)$ and $B(\geqslant 5)$, and low $T(\leqslant 1)$ and $B(\leqslant 1)$ where for attractive walls the chains begin to deposit on the walls. In both regimes, the monomer density profiles up to two or three lattice spacings from these walls are similar to the profiles for attractive walls. At high T and B, the monomer densities decrease at the walls, i.e., at $X=1000$, with its highest value at attractive walls and lowest at repulsive walls (Table I) as expected.

At low T and B where the adsorption transitions take place, the densities at the three wall are very different (see Table I). At attractive walls, the monomer density shoots up rapidly (from $X=998$ to $X=1000$) due to adsorption of the chains. At neutral walls, the densities do not vary much from the values two to three lattice spacings away (see Table I). At repulsive walls, on the other hand, the monomer density drops rapidly below its value in the bulk. At temperatures where strong adsorption occurs at the attractive walls $(T\leqslant 0.5)$, the monomer densities at repulsive walls drop to 0. There is no adsorption transition with neutral and repulsive walls. Thus, the type of wall, i.e., attractive, repulsive, or neutral is important in governing the density profile on the wall at low temperatures $T(\leqslant 1)$.

TABLE II. Exponent α in $p_d \sim L_c^{-\alpha}$ for chains in the bulk (α_B) and at attractive walls (α_W). Error bar on the order of ± 0.02.

Temperature T	Bias B	α_B	α_W
10.0	0.1	0.651	0.489
10.0	0.5	0.264	0.849
10.0	1.0	0.057	0.409
10.0	2.0	0.041	0.457
10.0	5.0	0.006	0.659
10.0	10.0	−0.026	0.979
5.0	0.1	0.623	0.928
5.0	0.5	0.044	0.374
5.0	1.0	0.013	0.367
5.0	2.0	0.059	0.512
5.0	5.0	0.047	0.91
5.0	10.0	0.15	1.039
1.0	0.1	0.17	−0.017
1.0	0.5	0.282	0.082
1.0	1.0	0.322	0.115
1.0	2.0	0.254	0.559
1.0	5.0	0.324	1.172
1.0	10.0	0.458	1.061
0.5	0.1	0.165	−0.025
0.5	0.5	0.318	−0.030
0.5	1.0	0.274	0.0
0.5	2.0	0.268	0.762
0.5	5.0	0.447	0.941
0.5	10.0	0.456	0.801
0.1	0.1	0.32	0.016
0.1	0.5	0.318	0.001
0.1	1.0	0.392	0.042
0.1	2.0	0.482	0.731
0.1	5.0	0.549	0.757
0.1	10.0	0.481	0.613

B. Variation of monomer density with L_c

Let us now examine a power-law dependence of the monomer density on chain length, $p_d \sim L_c^{-\alpha}$, which is observed at the wall and away from it in the bulk (Table II). This bulk regime, where the polymer density has reached its steady value in our observation time, is still close to the wall. We find that the power-law exponent (α) depends strongly on B and T but we have not attempted to quantify the dependence given the quality of the data since we do not see a simple monotonic variation of α with B and T over the whole parameter regime. However, the magnitudes of the exponent provide a measure of where the monomer density might depend strongly on chain length (i.e., the greater its magnitude, the greater the dependence), or not at all (as the magnitudes of the exponent tend to 0).

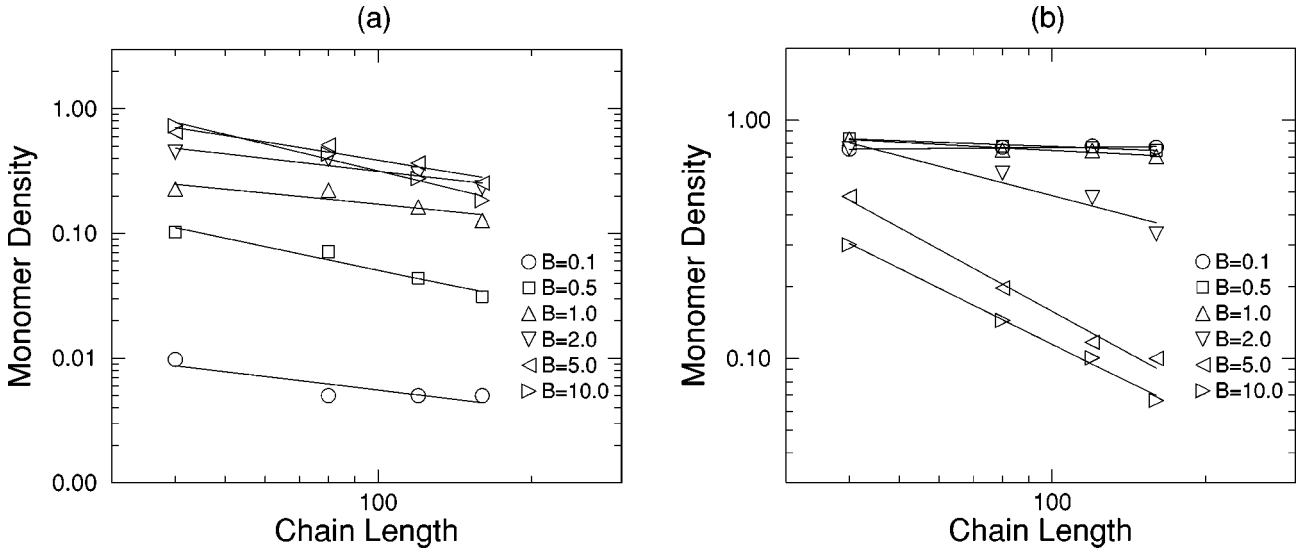

FIG. 7. Monomer density at the wall vs L_c at (a) $T=10$, (b) $T=1$.

In earlier sections, we have identified several regimes of B and T with their high and low magnitudes, and their corresponding effects on the chains in the bulk and at the wall such as layering effect/oscillations in density profile, and adsorption at the wall. These effects on the monomer density profiles are moderated by the length of the chains and their packing ability at a B and T. Thus, it is not surprising to find reflection of these regimes in the magnitude of exponent α. The exponents seem not to vary continually between regimes, but perhaps within regimes.

In the bulk, the field effectively drives and aligns the chains at high ($T(\geqslant 5)$, $B(\geqslant 5)$), and low ($T(\leqslant 1)$, $B(\leqslant 1)$) values of field and temperatures as seen before. In these field and temperature regimes, we find the lowest magnitudes of exponent (α) which increase as B decreases at high T and increases at low T. The increasing magnitudes of exponent indicate where the effect of field is too weak or interferes with alignment of chains such that packing constraints set by the chain (length) become important.

Chains at the wall (Fig. 7) show greater variations in the exponents α_W compared to chains in the bulk (Table II); note that there is more variation in α_W with B at low T than at high T. The small exponent values occur at low $T(\leqslant 1)$ and $B(\leqslant 1)$ where chains, regardless of length, are strongly adsorbed on wall. Note that chains are strongly driven to wall in this regime. In high T and B regime where chains are strongly driven, the exponent magnitudes at the wall generally increase with increasing B in contrast to exponent magnitudes in bulk which have decreasing trend. Thus in this regime, the packing of chains at the wall more severly depends on chain length and field. In other regimes (low T, high B and high T, low B) the exponents generally have large magnitude since fewer long chains are able to reach the wall compared to the shorter ones.

IV. WALL COVERAGE

At the wall, the number of sites oocupied by polymer nodes normalized by the total number of sites (i.e., the monomer density at the wall) gives the percentage coverage of the wall by polymer. This quantity provides a measure of the extent to which the polymer chains are adsorbed on the wall. Plots of the wall coverage versus T, B and L_c presented here show various regimes where the polymers are strongly/weakly adsorbed and the effects of these parameters on the coverage.

Variation of coverage with temperature is presented in Fig. 8. At low values of field $B(\leqslant 1.0)$ and low temperatures $T(<5.0)$, the coverage begins to increase rapidly as T decreases and tends to saturate to a maximum value at the lowest temperature ($T=0.1$) considered here. At $T=1$, it reaches above 80% for $L_c=40$ chains and 70% for $L_c=160$ chains. As temperature decreases further ($T\leqslant 0.5$), we find coverage exceeding 80% even for $L_c=160$ chains. The chains lie almost flat on the wall. As in a second order phase transition, on increasing the temperature, the coverage decays from nearly complete adsorption (at $T_a\sim 1$) down to nearly zero at the critical/transition temperature (T_c) where nearly complete desorption occurs. We have not attempted to estimate a more precise T_c, nevertheless, the adsorption-desorption transition temperature seems to depend on B and possibly on L_c. We would like to point out that a continuous transition was also observed by Lai recently.[19,20] We refrain from further studying the adsorption-desorption transition here due to difficulties in handling the large fluctuations in such a low dimension. As described in Sec. II, the chains are driven on a two dimensional plane and deposited on an impenetrable wall which is a line—this is a $(1+1)$ dimensional driven system, far from equilibrium. Therefore, adsorption-desorption transition at a linear wall is marred by large fluctuations. Such transition in higher dimensions (i.e., $(2+1)$) should have relatively less fluctuations and may be considered in our future studies.

At intermediate to high values of field ($B\geqslant 2$), the coverage of these chains exhibits a nonmonotonic dependence on T, achieving fairly high peak coverage (75%–80%) for $L_c=40$, and 25%–30% for $L_c=160$ at a characteristic tem-

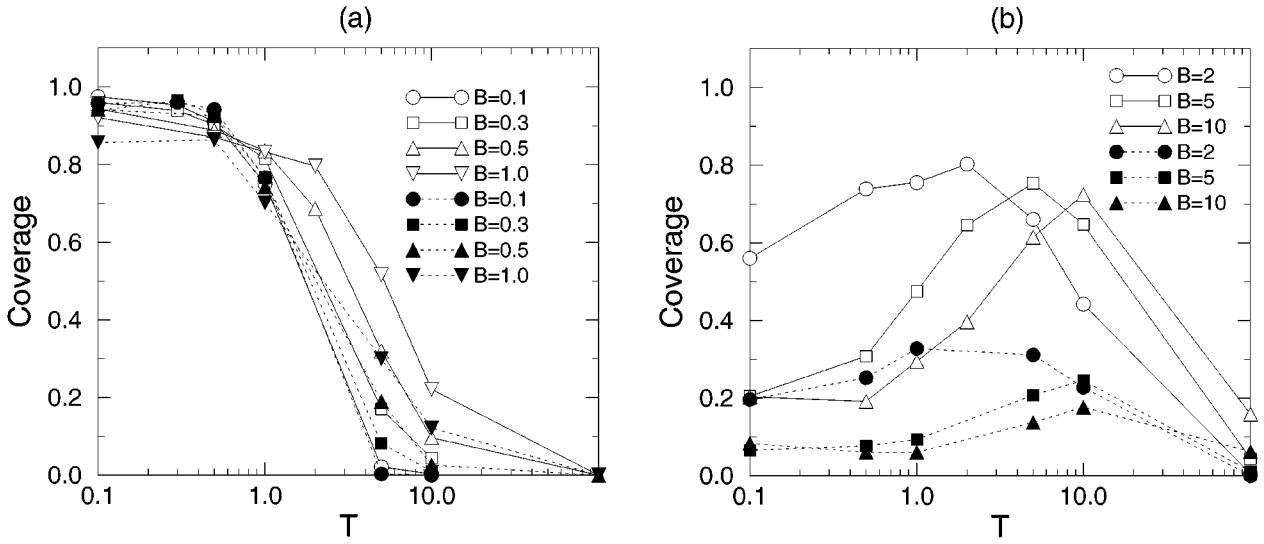

FIG. 8. Coverage vs T for $L_c=40$ (open symbol), 160 (filled symbol) chains at (a) low B, (b) high B.

perature (T_m) which increases with increasing B. We note that the peak coverage drops progressively as the chain length increases. The lower coverage is not unexpected as we have seen above, the longer elongated chains do not pack as densely as shorter ones. These temperatures lie in the range $T=1.0$ and $T=10.0$. At these high fields, the chains align in the field direction as in polymer brushes so the adsorption at the wall is mainly of the end segments of the polymer chains. The highest brush densities appear at about $T=2,5,10$ for $B=2,5,10$ respectively where $B/T\sim 1$. Thus, at high temperature, thermal energy dominates over the electrostatic energy. However, on lowering the temperature, the interaction energy becomes increasingly dominant over the thermal energy and the contact between chain nodes and wall increases with a maximum at T_m.

V. SUMMARY AND CONCLUSION

A Monte Carlo method was used to study the electrodeposition of interacting polymer chains on an impenetrable wall on a two dimensional discrete lattice. We explored the effects of temperature, field and chain length on the behavior of the monomer density profiles and coverage of chains at the wall with attractive, neutral, and repulsive interactions. The temperature and field compete in determining the movement of the chains particularly along the field direction. At high temperature, high fields are necessary to drive the chains more effectively toward the wall while at low temperature, low fields are quite effective. The interplay between the field and the effect of wall aligns the chains along the field (x-)direction and induces a layering effect. Consequently oscillations appear in the monomer density profile along the x axis. These oscillations occur above a characteristic value of bias B_c which depends on chain length and temperature. Generally, the value of B_c beyond which the oscillations are observed decreases with increasing chain length and/or decreasing temperature.

For attractive walls, a nearly complete adsorption is observed at low $T(\leqslant 1)$ and low $B(\leqslant 1)$. At the same values of B, on increasing the temperature the coverage drops down to nearly zero at a critical temperature (T_c) leading to a complete desorption. Thus, at low B, we observe an adsorption at low T and desorption at high T with an adsorption-desorption transition consistent with the recent simulations in different model systems. In high field ($B\geqslant 2.0$), we find that the coverage depends non-monotonically on temperature with a maximum value at a characteristic temperature (T_m) which increases on increasing the field. At high temperature, coverage at the walls depends strongly on chain length. Short chains are able to pack more densely than longer ones as they align under the influence of field, resulting in a higher coverage. Equilibrium polymer density at the wall and away from it (i.e., in the bulk) shows a power-law decay with the chain length, $p_d\sim L_c^{-\alpha}$; the power-law exponent α depends on the magnitude of the field and temperature with the range of values 0.0-1.0 at the wall and 0.0-0.65 in the bulk. No adsorption transitions occur for neutral and repulsive walls. At neutral walls, the monomer density is almost unchanged from its value near the wall. However, at repulsive walls there are almost no monomers.

ACKNOWLEDGMENTS

This work is supported by a NSF-EPSCoR grant. G.M.F. acknowledges support for computer time at the CADCAM and Computer Center of the National University of Singapore.

[1] *Dynamics of Fractal Surfaces*, edited by F. Family and T. Vicsek (World Scientific, Singapore, 1991).
[2] A. L. Barabasi and H. E. Stanley, *Fractal Concepts in Surface Growth* (Cambridge University Press, Cambridge, 1995).
[3] J. Y. Tsao, *Materials Fundamentals of Molecular Beam Epitaxy* (Academic, San Diego, 1993).
[4] G. J. Fleer, M. A. Cohen Stuart, J. M. H. M. Scheutjens, T. Cosgrove, and B. Vincent, *Polymers at Interfaces* (Chapman and Hall, London, 1993).

[5] E. Eisenriegler, *Polymers Near Surfaces* (World Scientific, Singapore, 1993).
[6] S. A. Safran, *Statistical Thermodynamics of Surfaces, Interfaces, and Membranes* (Addison–Wesley, Reading, 1994).
[7] R. P. Wool, *Polymer Surfaces: Structure and Strength* (Hanser, New York, 1995).
[8] *Graphics and Animation in Surface Science*, edited by D. D. Vvedensky and S. Holloway (IOP, Bristol, 1992).
[9] S. D. Sarma and P. Tamborena, Phys. Rev. Lett. **66**, 325 (1991).
[10] D. E. Wolf and J. Villain, Europhys. Lett. **13**, 389 (1990).
[11] S. Pal and D. P. Landau, Phys. Rev. B **49**, 10597 (1994).
[12] G. S. Grest, Phys. Rev. Lett. **76**, 4979 (1996).
[13] G. S. Grest, J. Chem. Phys. **105**, 5532 (1996).
[14] H. Kallabis and M. Lassig, Phys. Rev. Lett. **75**, 1578 (1995).
[15] R. B. Pandey, A. Milchev, and K. Binder, Macromolecules **30**, 1194 (1997).
[16] U. D'Ortona, J. D. Coninck, J. Koplik, and J. R. Banavar, Phys. Rev. Lett. **74**, 928 (1995).
[17] U. D'Ortona, J. D. Coninck, J. Koplik, and J. R. Banavar, Phys. Rev. E **53**, 562 (1996).
[18] R. Zajac and A. Chakrabarti, J. Chem. Phys. **104**, 2418 (1996).
[19] P. Y. Lai, Phys. Rev. E **49**, 5420 (1994).
[20] P. Y. Lai, J. Chem. Phys. **103**, 5742 (1995).
[21] J. Baschnagel and K. Binder, Macromolecules **28**, 6808 (1995).
[22] A. Milchev and K. Binder, Macromolecules **29**, 343 (1996).
[23] E. Bouchaud and M. Daoud, J. Phys. A **20**, 1463 (1987).
[24] E. Eisenriegler, K. Kremer, and K. Binder, J. Chem. Phys. **77**, 6296 (1982).
[25] G. ten Brinke, D. Ausserre, and G. Hadziioannou, J. Chem. Phys. **89**, 4374 (1988).
[26] G. M. Foo and R. B. Pandey, Phys. Rev. Lett **79**, 2903 (1997).